SYNTHETIC JETS IN CROSS-FLOW
PART II: JETS FROM ORIFICES OF DIFFERENT GEOMETRY

Ivana M. Milanovic*
University of Hartford
West Hartford, Connecticut 06117

K. B. M. Q. Zaman†
National Aeronautics and Space Administration
Glenn Research Center
Cleveland, Ohio 44135

ABSTRACT

The flow fields of synthetic jets in a cross-flow from orifices of different geometry are investigated. The geometries include a straight, a tapered, a pitched and a cluster of nine orifices, all having the same cross-sectional area through which the perturbation is discharged into the cross-flow. The 'strength' of the jet from the tapered orifice in comparison to that from the straight one is found to be only slightly enhanced. The flow field from the cluster of orifices, when viewed a few equivalent diameters downstream, is similar to that from the single orifice. However, the penetration is somewhat lower in the former case due to the increased mixing of the distributed jets with the cross-flow. The penetration for the pitched configuration is the lowest, as expected. The jet trajectories for the straight and pitched orifices are well represented by correlation equations available for steady jets-in-cross-flow. Distributions of streamwise velocity, vorticity as well as turbulence intensity are documented for various cases. In addition, distributions of phase-averaged velocity and vorticity for the cylindrical and the clustered orifices are presented providing an insight into the flow dynamics.

INTRODUCTION

This is a companion paper of the work reported in Ref. 1. The motivation, objective and the scope of the study together with a literature review on the flow dynamics of isolated synthetic jets have been described previously[1] and will not be repeated. Here, a brief additional overview of experiments on synthetic jets in the cross-flow (SJCF) examining the effects of orifice geometry is presented. The study by Chen et al.[2] observed an improved mixing with the cross-flow when using an array of synthetic jets. Smith et al.[3] reported a deeper penetration of SJCF compared to that of a continuous jet in cross-flow (JICF) with comparable velocity ratio. Bridges and Smith[4] investigated the interaction between a synthetic jet and a turbulent boundary layer while varying the orientation of a rectangular orifice. Increased turbulence intensity in the boundary layer was observed when the major axis of the orifice was at an angle with the free stream. Smith[5] explored the interaction between an array of synthetic jets exiting from rectangular orifices and a turbulent boundary layer. In the 'streamwise configuration' where major axis was aligned with the cross-flow the velocity profiles were similar to those measured in a JICF. The jet trajectory for the 'spanwise configuration' was found to follow the power law of a JICF. Gordon and Soria[6] studied circular synthetic jets in cross-flow with particle image velocimetry, and compared them to continuous and pulsed counterparts. The results suggested similarity of SJCF to free synthetic jets in the near field ($y < 3D$) and to pulsed jets farther downstream. Jet penetration was within the range reported for continuous JICF. Flow visualization study of Watson et al.[7] addressed optimum spacing between twin synthetic jets with and without the cross-flow. Combined effect of orifice spacing and angle between the axis connecting orifices and the freestream was shown to influence the amount of mixing.

However, in spite of the studies reviewed above, it is fair to infer that a satisfactory database and full understanding of SJCF from orifices of different geometry are far from complete. The present study is another effort towards those objectives. Detailed time- and phase-averaged flow-field properties are presented for selected orifice

* Member AIAA, Assistant Professor
† Associate Fellow AIAA, Aerospace Engineer

geometries. The configurations, experimental conditions and parametric ranges are described next.

EXPERIMENTAL SETUP

The orifice geometries are shown schematically in Fig. 1. These are cut in a 10 in. diameter x 1 in. thick clear plastic plate that is mounted flush on the test section floor. The orifices include: (1) a straight cylindrical one with diameter, D = 0.75 in., (2) a cluster of nine each with diameter, d = 0.25 in., and spaced 2d apart, (3) a slanted one of diameter, D = 0.75 in., pitched at $\alpha = 20^{\circ}$ relative to the floor of the test section, and (4) one tapering from 1 in. to 0.75 in. diameter. Thus, the equivalent diameter based on the area of cross-section through which the flow perturbation discharged into the cross-flow was the same for all cases, D = 0.75 in.

Most of the measurements were done for a cross-stream velocity of U_∞ = 20 ft/s. With the momentum flux ratio (J) previously defined[1] in terms of the maximum jet velocity and the cross-flow velocity, $J = \left(V_{max}/U_\infty\right)^2$, J values in the current investigation were up to 6.

The method for acquiring the velocity amplitude, V_0, and the stroke length, L_0, was the same as described in Ref. 1. Velocity profiles at different streamwise locations, x, on the symmetry plane (z = 0) were obtained with a single element hot-wire. These measurements included the fundamental amplitude u'_f (r.m.s. level at the perturbation frequency) obtained by 'on-line' spectral analysis. Two ×-wires were used to map the flow on cross-sectional planes at x/D = 0.5, 5 and 10. The data provided all three components of velocity, turbulent stresses and streamwise vorticity on a time-averaged basis. In addition, phase-averaged velocities and streamwise vorticity were also obtained at x/D = 5 for the cylindrical and the clustered cases.

RESULTS

Figure 2 shows mean centerline velocity 5D away from the exit, without the cross-flow. For the slanted orifice, the probe was placed on the pitch axis, while for the clustered configuration the probe was on the axis of the central hole. One finds that the response to the perturbation is very similar for the (straight) cylindrical, tapered and the clustered cases. A scrutiny reveals that the velocity is somewhat higher for the tapered geometry. Comparison of other properties (e.g., u'_f versus frequency) also showed slightly stronger response for the tapered orifice. However, the differences were minor and the tapered configuration was not pursued any further in this study.

The data in Fig. 2 also reveal a weaker response for the clustered case relative to the single orifice. This is expected due to the distribution of the holes and more boundary layer flow involved in the cluster. In fact, it is surprising that the aggregate effect for the cluster is so close to that for the single orifice.

The velocities in Fig. 2 are the smallest for the pitched orifice. The main reason for this appears to be the resonance characteristics of the cavity-orifice configuration. The Helmholtz resonance was calculated and verified by cursory measurements. For the cylindrical, tapered and clustered arrangement it was found to be approximately 25 Hz. Thus, for those three geometries, in Fig. 2, the perturbation was at the resonant frequency. For the pitched orifice, due to the increased length, the resonance frequency is lower, about 18 Hz. Therefore, for same input voltage the amplitude is the least for the pitched case due to off-resonant condition. It should be noted that the Helmholtz resonance simply provides a means to impart large amplitude perturbation. As found by previous researchers and in Ref. 1, the synthetic jet characteristics are governed by the stroke length (L_0/D) and momentum flux ratio (J) regardless of the resonance condition. All results presented in the following pertain to a frequency, f = 25Hz, and input voltage, A = 9.6V. The resulting stroke length and momentum flux ratio are 19.9 and 6, respectively.

With the cross-flow on, flow properties obtained at x/D = 10 on the symmetry plane are compared in Fig. 3 for the cylindrical, clustered and pitched orifices. Mean velocity (U) profiles shown in (a) indicate a 'stronger' response for the pitched configuration. Recall from Fig. 2 that for same input voltage the perturbation amplitude is actually the lowest for this orifice. Yet higher U is measured simply because the pitch geometry directs the synthetic jet along the cross-flow at an angle of only 20°. The turbulence and fundamental intensities, shown in Figs. 3(b) and (c), also exhibit accentuated values for the pitched case.

The location of the peak in u'_f–profile (y_{max}) was used to denote the penetration of the SJCF.[1] As expected, one finds from Fig. 3(c) that y_{max} is the least for the pitched configuration. For the cluster, y_{max} is also smaller than that for the cylindrical orifice. Recall from Fig. 2 that the velocity without the cross-flow was about the same for the latter two geometries. The less penetration of the SJCF for the clustered case is apparently due to an increased mixing of the distributed jets with the cross-flow.

Values of u'_f only, measured at different x/D are compared in Fig. 4 for the three geometries of Fig. 3. There is a systematic shift of the peak in u'_f-profiles with

increasing x. The y_{max} data obtained from these profiles are shown in Fig. 5 for the cylindrical and the pitched orifices. The u'_f -peak locations for the clustered configuration were ambiguous and thus are not shown. However, the profiles in Fig. 3 already indicated that the jet penetration is less for the clustered case. This is also confirmed with the cross-sectional surveys as discussed later.

In Fig. 5, the trajectories of the SJCF are compared with those obtained from the equation,

$$\frac{y_{max}}{D} = \left(\frac{x}{D}\right)^{0.33} J^{0.43} \sin\alpha ,$$

which represents the correlation for the penetration of a steady jet-in-cross-flow.[8] For the straight and clustered geometries α = 90°. As defined earlier, J for the SJCF is the square of the ratio of the maximum discharge velocity to cross-flow velocity. It can be seen that the trajectories of the SJCF follow the correlation for the continuous JICF well, even for the pitched case, provided that y_{max} and J are defined as stated.

The evolution of the SJCF for the cylindrical orifice is illustrated in Fig. 6 with mean streamwise velocity contours. A kidney-shaped distribution of high velocity fluid is observed at the location closest to the exit. However, farther downstream the flow-field is characterized mainly by a dome of low velocity fluid pulled from the boundary layer. A similar distribution is seen for the clustered case, shown in Fig. 7. Once again, the clustered configuration is remarkable in that the effect from the nine orifices becomes an aggregate, as if the SJ was issuing from a single orifice. Also, as indicated before, the jet penetration for the clustered geometry is somewhat lower than that of the cylindrical case. It is also noted that the lateral spreading at the farthest x is actually smaller for the clustered case even though the holes are distributed over a larger area.

The corresponding velocity distributions for the pitched case are presented in Fig. 8. There is a noteworthy difference with the other two configurations. Instead of a dome of low velocity fluid here a higher velocity core is observed around the symmetry plane, near the wall. Even at x/D = 10 this high-velocity core has neither lifted up nor distorted into the 'kidney-shape'. It is apparent that the jet pitched at 20° behaves similar to a 'wall-jet' within the measurement domain covered in the experiment. It should be noted that the legend bars with all the field data provides an idea about the maximum and minimum amplitudes in the field.

Turbulence intensity distributions obtained at x/D = 5 are compared in Fig. 9. The vertical extent of the flow-field structures is commensurate with jet penetrations discussed earlier with the mean velocity data. Note that corresponding U-contours are shown as part (b) of Figs. 6-8. All three orifice configurations have regions of highest turbulence intensity near the symmetry plane. In the case of cylindrical and clustered geometries, these areas coincide with the domes of low momentum fluid. For the pitched configuration, high turbulence zone overlaps with the core of high momentum fluid. The former two cases also have a region of high turbulence in the boundary layer directly underneath.

Contour plots of streamwise vorticity corresponding to Fig. 9 are shown in Fig. 10. In each case a pair of counter-rotating vortices, similar to the 'bound vortex pair' of a steady jet-in-cross-flow, is observed. Not surprisingly this structure is the weakest for the pitched geometry since the jet has not lifted up. It is unexpected, however, that the pair is considerably stronger for the clustered arrangement relative to the single orifice. In addition to the 'bound vortex pair', the cylindrical case in particular features another one near the wall having an opposite sense. The magnitude of vorticity in the latter pair is significantly higher. Phase-averaged data are presented next in an effort to glean further insight into these flow fields.

Distributions of phase-averaged properties were obtained with the same ×-wire survey scheme, using the input to the woofer as a reference. The zero-crossings of the reference signal with positive slopes were used as triggers.[1] Data were acquired for 19 phases within the period of perturbation. Phase-averaged streamwise velocity contours at x/D = 5 are shown for the cylindrical case in Fig. 11. The eight figures are approximately at equal intervals covering the period. The phases on the left represent the 'discharge' segment of the cycle, while those on the right represent 'suction'. These data capture the unsteady cycling of the synthetic jet in the cross-flow and provide a clear perspective of the events leading to the time-averaged field seen in Fig. 6(b). Corresponding phase-averaged data for the clustered case are shown in Fig. 12. One notes somewhat more complex changes in the flow field within the cycle. The events take place closer to the wall leading to a lesser penetration of the SJCF on a time-averaged basis (Fig. 7b), compared to the cylindrical case.

Finally, phase-averaged streamwise vorticity contours for the cylindrical orifice only are shown in Fig. 13. These correspond to the phases of Fig. 11. One notes that the

bound vortex pair can be much stronger at certain phases within the period. Peak levels are more than three times that seen in the time-averaged field (Fig. 10a). During the suction half of the cycle the bound vortex-pair is absent, as expected. However, at all phases, throughout discharge as well as suction, another pair of vortices is seen near the wall. It has a sense opposite to that of the bound vortex pair and shows up in the time-averaged field discussed earlier with Fig. 10.

It is not clear if there would be a similar pair near the wall for a steady jet-in-cross-flow counterpart. The value of momentum flux ratio yielding same trajectory as discussed in conjunction with Fig. 5, is about 6. Unfortunately, vorticity was not measured for a steady JICF with comparable J in this investigation and corresponding data could not be found in the literature. However, the secondary vortex structure was not observed at a higher momentum flux ratio ($J = 44$).[9] Thus, the additional vortex pair near the wall could be a feature of SJCF different from the steady JICF. It appears that reorientation of the approach boundary layer is responsible for this. While the bound vortex-pair appears only during the discharge part of the cycle, the 'horse-shoe' pair is present during discharge as well as suction. It might be absent only at the exact phases when the velocity at the orifice exit is zero. In any case, its occurrence at most phases results in vorticity levels higher than the bound vortex pair. This was seen in Fig. 10.

CONCLUSIONS

Results of an experimental investigation on synthetic jets from orifices of different geometry with and without cross-flow are presented. The main conclusions are enumerated in the following.

(1) Just a few equivalent diameters downstream, the SJCF from the cluster of orifices is found to be quite similar to that from the single orifice.

(2) Jet penetration is somewhat less for the cluster in comparison with the isolated orifice due to increased mixing with the cross-flow. As expected, the jet penetration is the least for the pitched geometry.

(3) The trajectories of the SJCF follow correlation equations available for steady JICF.

(4) The mean velocity distributions for the single and clustered orifices are mainly characterized by a dome of low-momentum fluid pulled up from the boundary layer. In contrast, the velocity field for the pitched case involves a region of high-momentum fluid occurring near the wall and around the symmetry plane, similar to a 'wall jet'.

(5) The domes of low momentum fluid in the single and cluster cases and the region of high momentum fluid in the pitched case also coincide with regions of highest turbulence intensities.

(5) The streamwise vorticity distribution is characterized by a 'bound vortex pair' typical of a steady jet-in-cross-flow. For the single orifice, in addition to the bound vortex pair, another pair with opposite sense occurs directly underneath near the wall. It is inferred that the latter pair is due to the reorientation of the approach boundary layer.

ACKNOWLEDGEMENTS

The work was supported by NASA-OAI Collaborative Aerospace Research and Fellowship Program. The second author is grateful to Connecticut Space Grant College Consortium - EPSCoR Core Funding for providing support. The authors are also thankful to Dr. Gerard E. Welch of US Army for valuable inputs.

REFERENCES

1. Zaman, K.B.M.Q., and Milanovic, I. M., "Synthetic Jets in Cross-flow. Part 1: Round jet", AIAA Paper 03-0000, AIAA 33rd Fluid Dynamics Conference Orlando, FL, June 2003.
2. Chen, Y., Liang, S., Aung, K., Glezer, A., and Jagoda, J., "Enhanced Mixing in a Simulated Combustor Using Synthetic Jet Actuators", AIAA Paper 99-0449, 37th Aerospace Sciences Meeting and Exhibit, Reno, NV, January 1999.
3. Smith, D. R., Kibens, V. Pitt, D. M., and Hopkins, M. A., "Effect of Synthetic Jet Arrays on Boundary Layer Control", SPIE Paper 3674-45, 6th International Symposium on Smart Structures and Materials.
4. Bridges, A., and Smith, D. R., "The Influence of Orifice Orientation on the Interaction of Synthetic Jet with a Turbulent Boundary Layer", AIAA 2001-2774, 31st AIAA Fluid Dynamics Conference and Exibit, Anaheim, CA, June 2001.
5. Smith, D. R., "Interaction of a Synthetic Jet with a Crossflow Boundary Layer", *AIAA Journal*, 40 (11): 2277-2288, 2002.
6. Gordon, M., and Soria, J., "PIV Measurements of a Zero-Net-Mass-Flux Jet in Cross Flow," *Experiments in Fluids*, 33: 863-872, 2002.
7. Watson, M., Jaworski, A. J., and Wood, N. J., "Contribution to the Understanding of Flow Interactions Between Multiple Synthetic Jets", *AIAA Journal*, 41 (4): 747-749, 2003.
8. Abramovich, G. N., "The Theory of Turbulent Jets", The M.I.T. Press, 1963.
9. Zaman, K.B.M.Q., "Effect of Oscillating Tabs on a Jet-in-Cross-Flow", AIAA Paper 03-0632, 41st Aerospace Sciences Meeting, Reno, NV, January 2003.

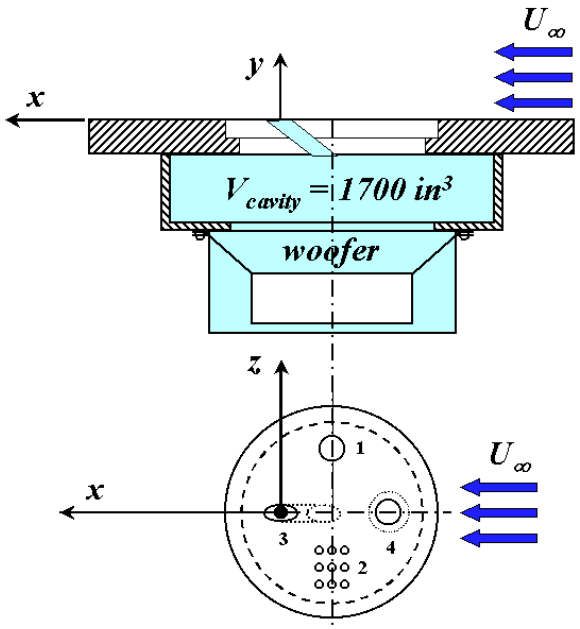

Fig. 1 Experimental set up and orifice configurations:
(1) cylindrical, (2) clustered, (3) pitched, (4) tapered.

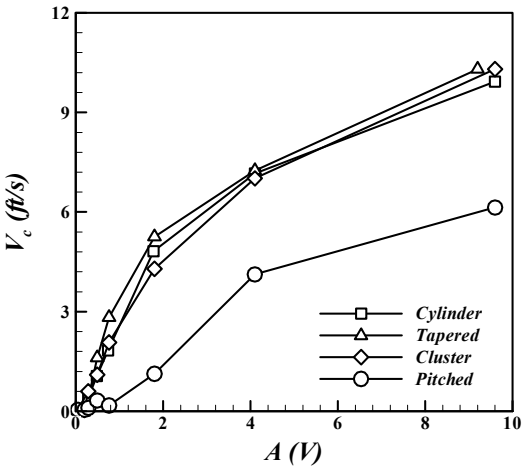

Fig. 2 Mean centerline velocity versus amplitude of excitation for SJ's without cross-flow for different orifice configurations; $y/D = 5$, $z/D = 0$, $f = 25$ Hz, $U_\infty = 0$.

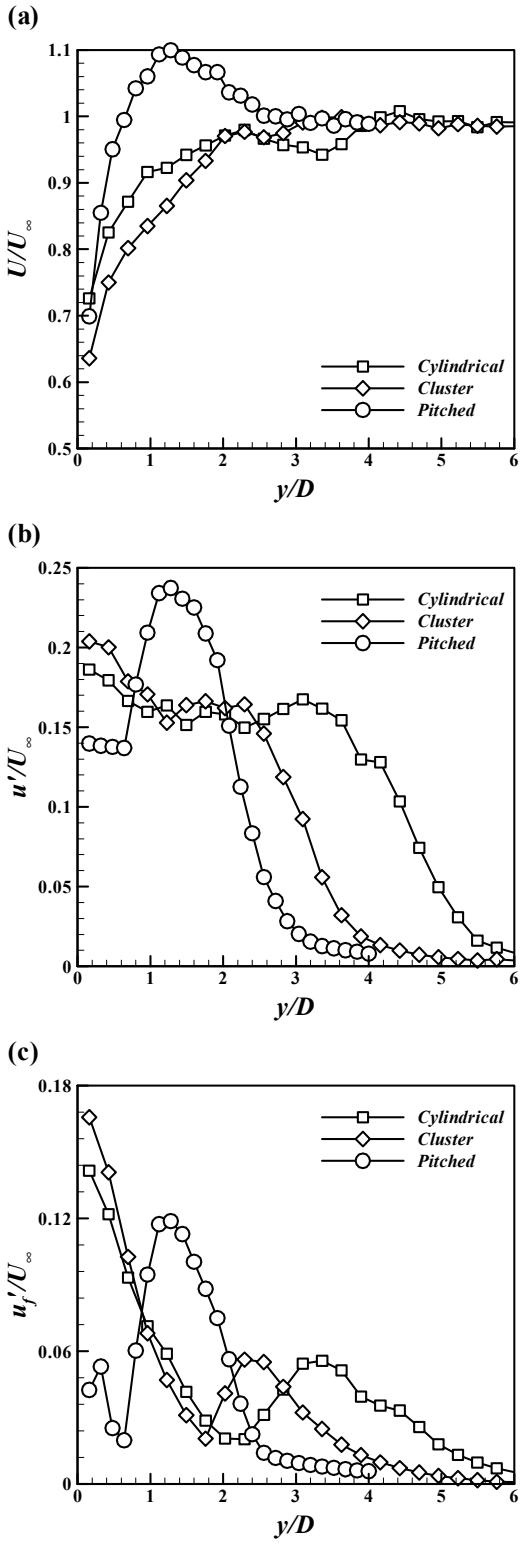

Fig. 3 Streamwise mean and fluctuating velocity profiles for SJCF, x/D = 10, z/D = 0; (a) Mean velocity, (b) Turbulence intensity, (c) Fundamental (r.m.s.) intensity.

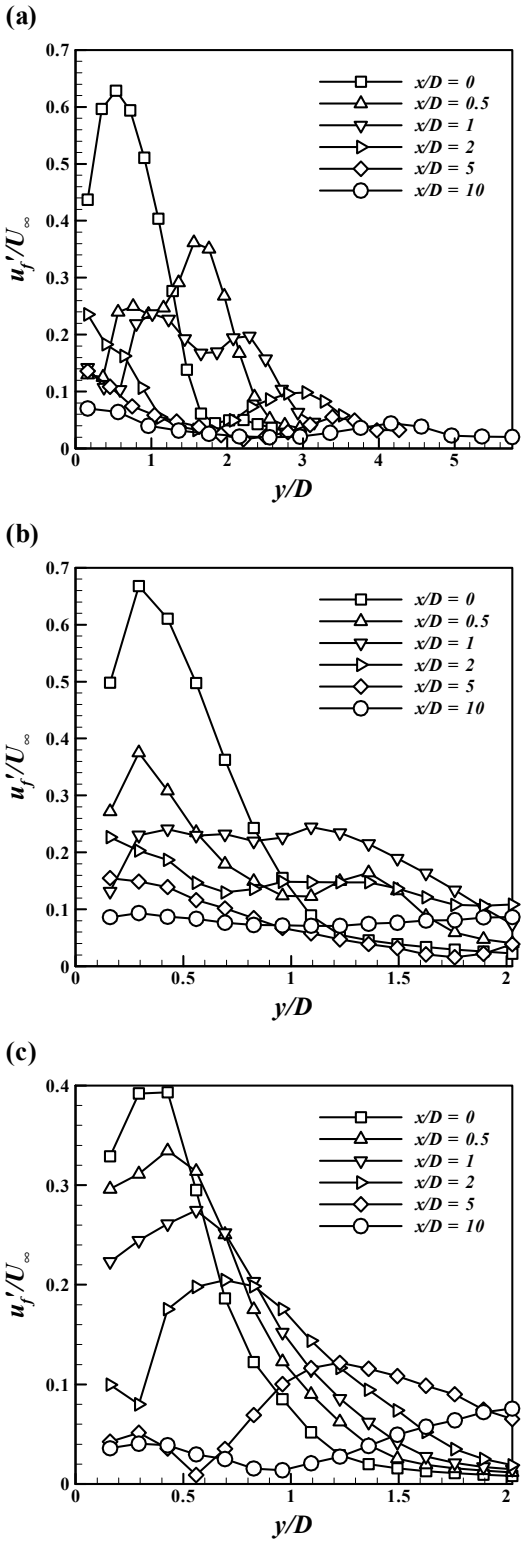

Fig. 4 Profiles of fundamental (r.m.s.) intensity at indicated downstream (x/D) locations, z/D = 0; (a) Cylindrical, (b) Clustered, (c) Pitched case.

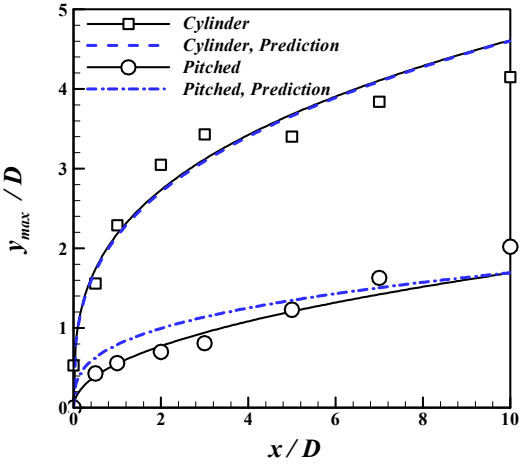

Fig. 5 SJ trajectory, based on u'_{fmax}, for cylindrical and pitched cases; $z/D = 0$.

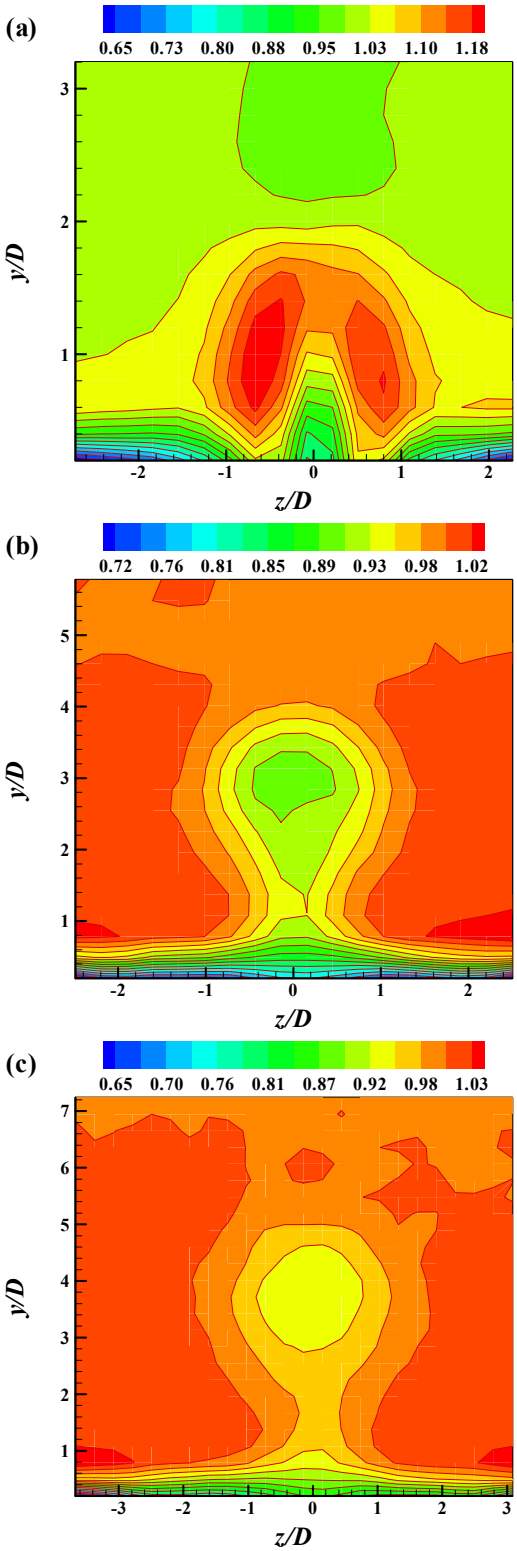

Fig. 6 Streamwise mean velocity contours for SJCF from cylindrical orifice; (a) $x/D = 0.5$, (b) $x/D = 5$, (c) $x/D = 10$.

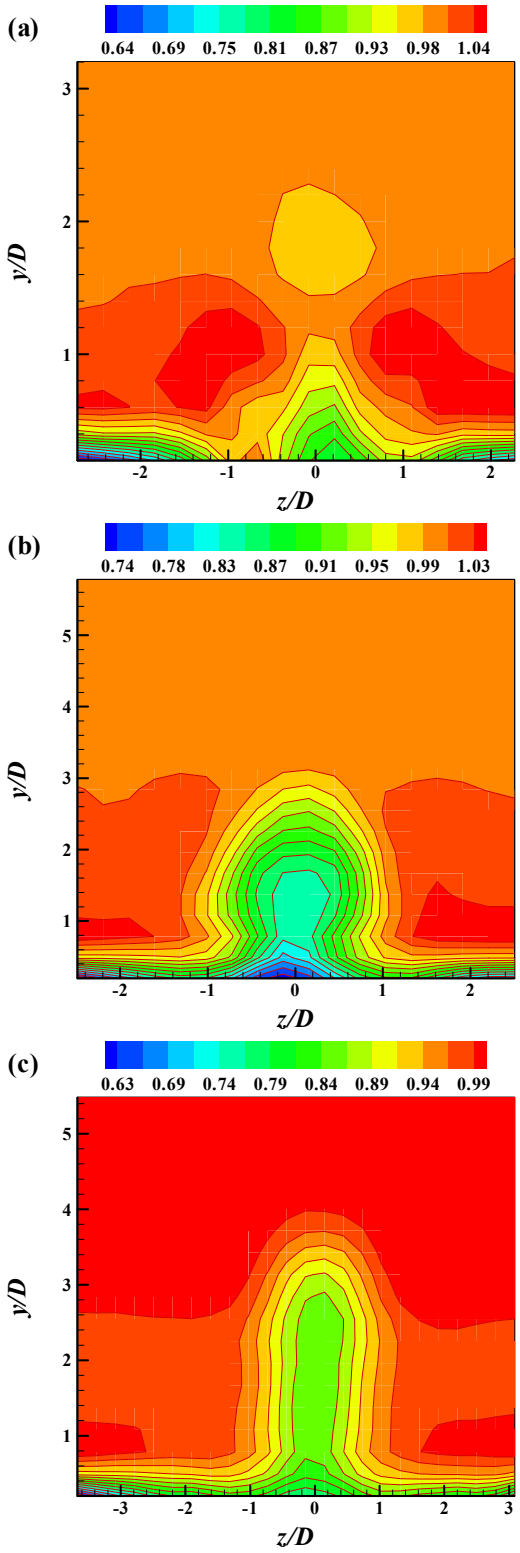

Fig. 7 Streamwise mean velocity contours for SJCF from clustered orifice; (a) x/D = 0.5, (b) x/D = 5, (c) x/D = 10.

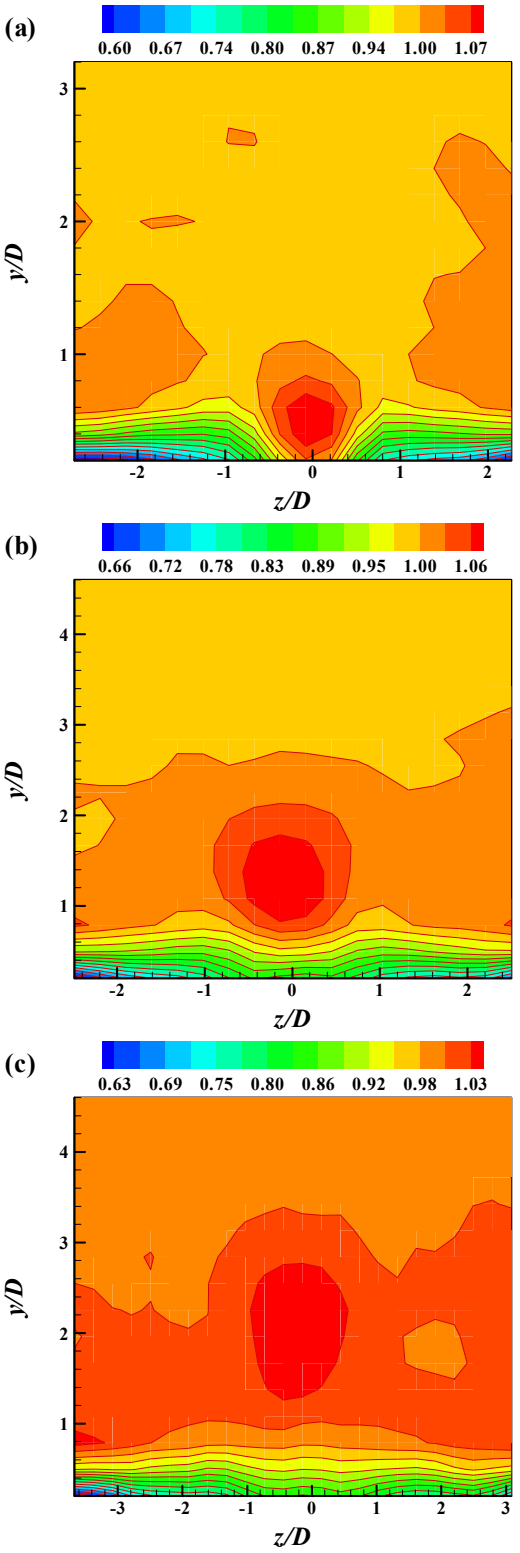

Fig. 8 Streamwise mean velocity contours for SJCF from pitched orifice, α = 20^0; (a) x/D = 0.5, (b) x/D = 5, (c) x/D = 10.

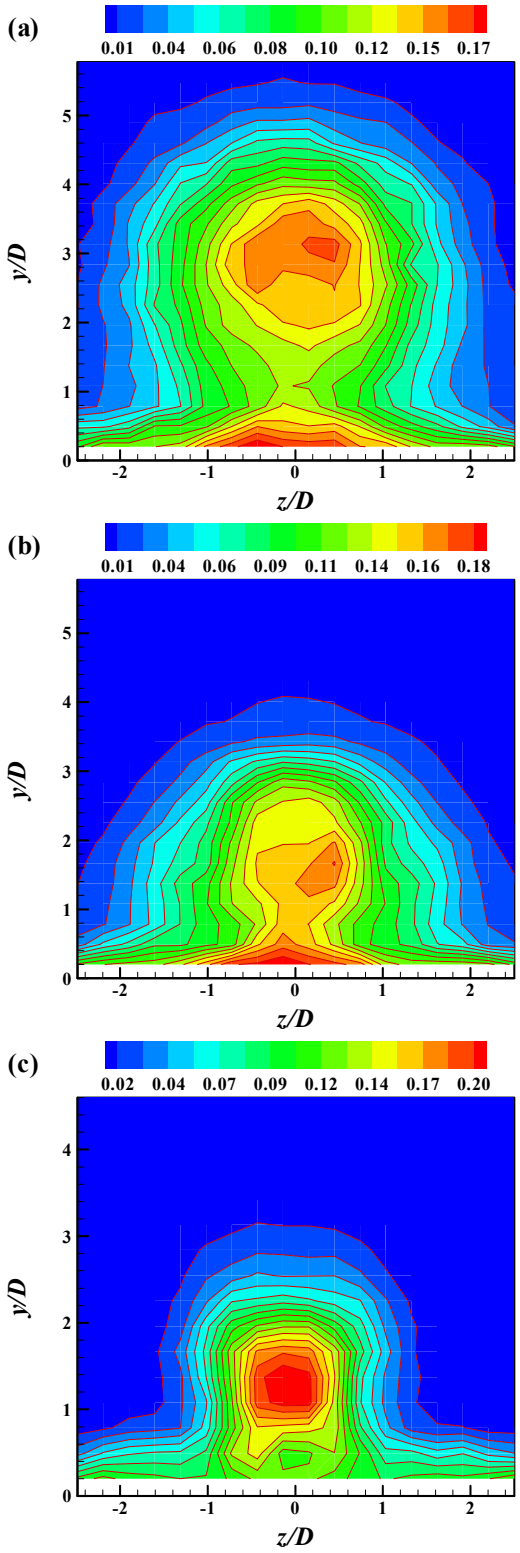

Fig. 9 Streamwise contours of turbulence intensity, x/D = 5; (a) Cylindrical, (b) Clustered, (c) Pitched case.

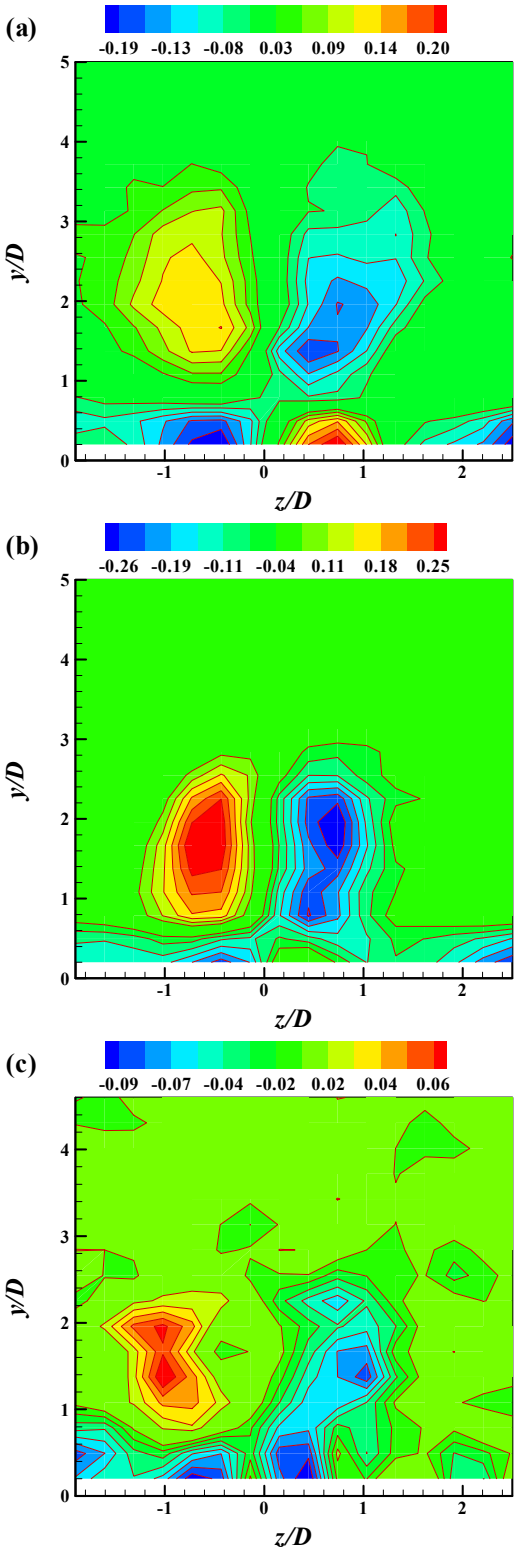

Fig. 10 Streamwise mean vorticity contours, x/D = 5. (a) Cylindrical, (b) Clustered, (c) Pitched case.

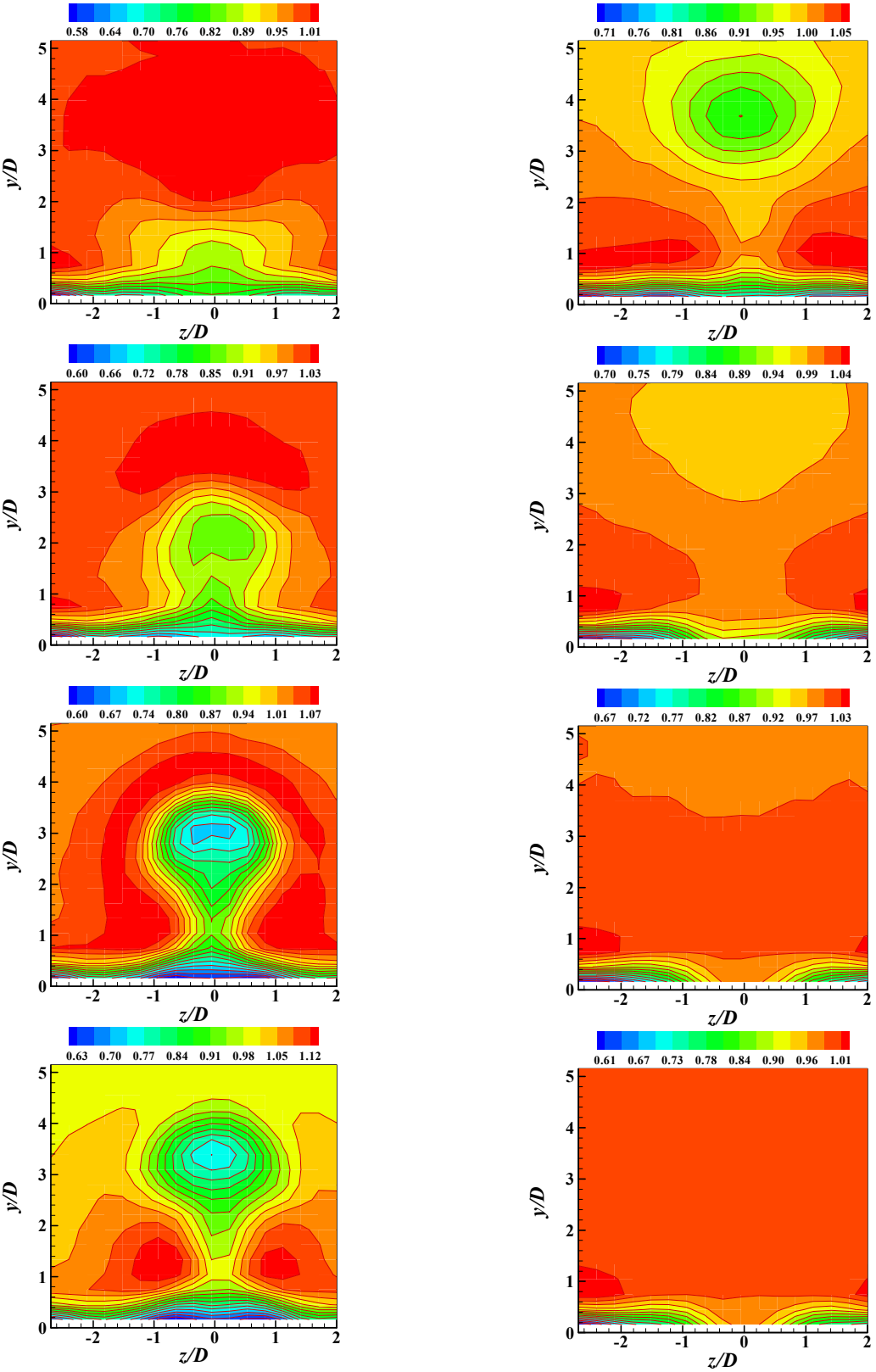

Fig. 11 Phase-averaged streamwise vorticity contours for SJCF from cylindrical orifice, x/D = 5. The eight figures are at equally spaced phases within the excitation period.

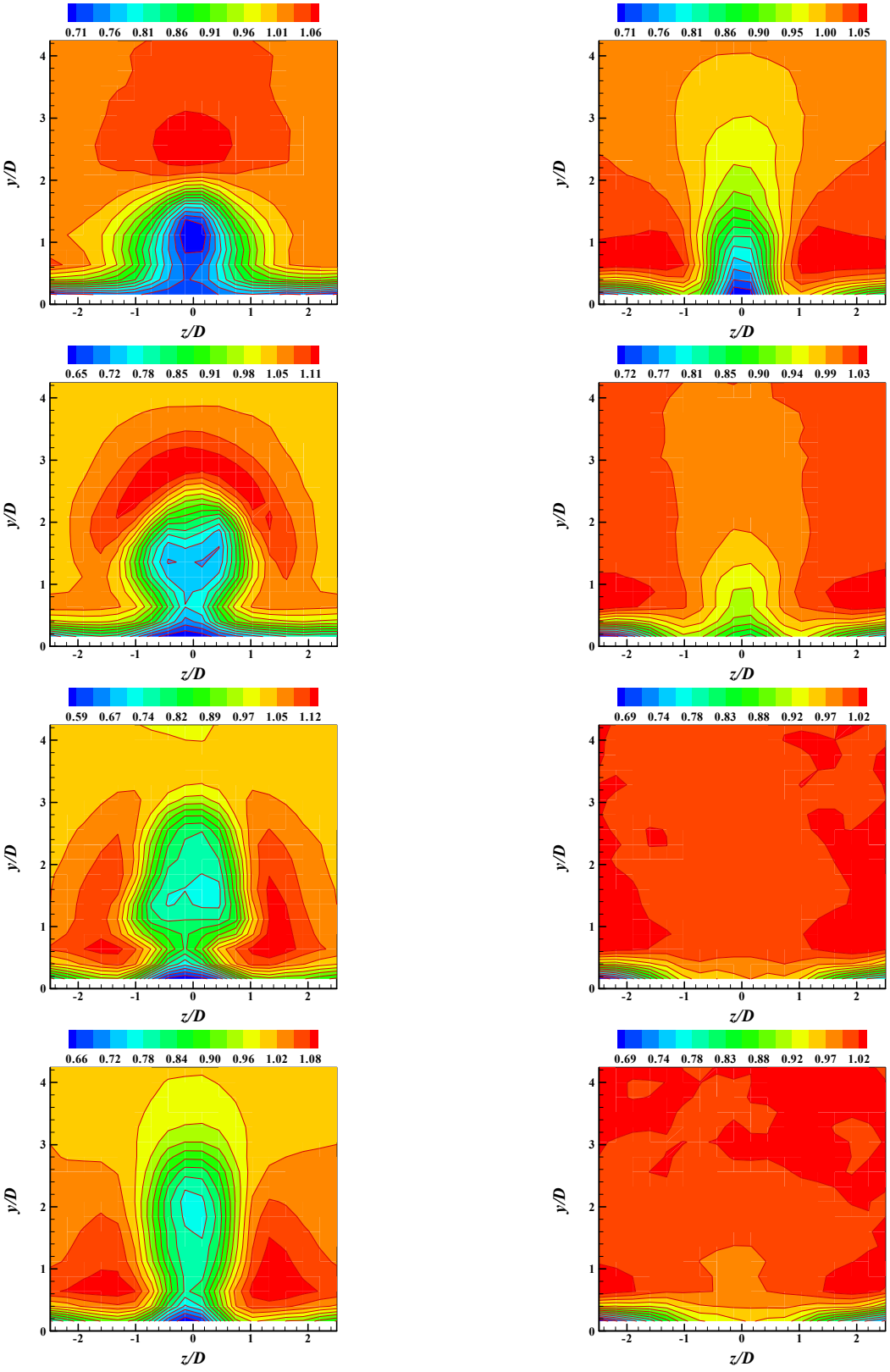

Fig. 12 Phase-averaged streamwise vorticity contours for SJCF from clustered as in Fig. 11, $x/D = 5$.

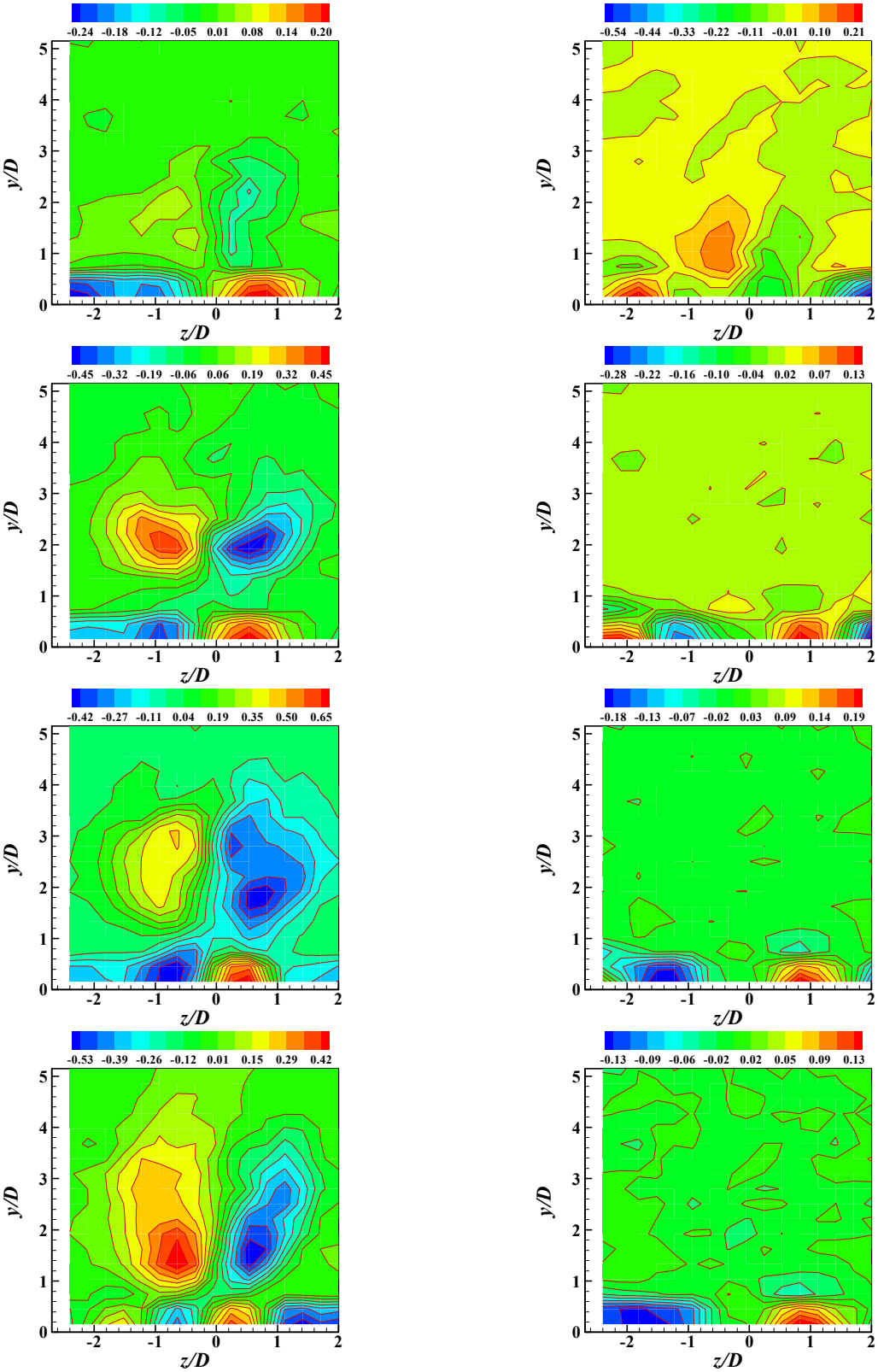

Fig. 13 Phase-averaged streamwise vorticity contours for SJCF from cylindrical orifice corresponding to the data of Fig. 11.